Alma Mater Studiorum Università di Bologna
Archivio istituzionale della ricerca

Dynamic Ray Tracing: Introduction and Concept

(Article begins on next page)

30 November 2024

Dynamic Ray Tracing: Introduction and Concept

D. Bilibashi, E. M. Vitucci, V. Degli-Esposti

Abstract — **Radio applications in vehicular environment are becoming popular due to the development of autonomous driving and safety enforcement technologies that make use of vehicle-to-vehicle, vehicle-to-infrastructure as well as of radar solutions. Due the large variety of possible environment configurations, and to the highly dynamic characteristics of the environment, specific deterministic radio propagation models must be developed to assist the design and simulation of such vehicular applications. In the present work we present a dynamic ray tracing model that can provide a multidimensional channel prediction, including Doppler's shifts, with a single run on the base of a suitable "dynamic environment database" that describes a scene with moving objects and terminals. The proposed approach applied to a reference street canyon scenario with a large moving object representing a bus is shown to yield realistic estimates of the channel's power-Doppler profiles.**

Index Terms — **Ray Tracing, Millimeter wave propagation, Vehicular Ad Hoc Networks, Doppler Effect, Mobile Radio Mobility, 5G Mobile Communications**

I. INTRODUCTION

Ray tracing radio propagation models have been developed over the last three decades and used for the design and deployment of cellular radio systems [1][2].

Recently, radio applications in vehicular environment have gained popularity with the development of autonomous driving and of wireless systems for traffic control and safety enforcement, such as vehicular applications of 5th Generation (5G) systems and automotive radar solutions [3][4][5]. Extensive work on vehicular channel measurement and modeling has been carried out in the last years [6][7], including the development of deterministic ray-based models for vehicular environment [8] [9].

With the advent of millimeter-wave (mm-wave) frequency bands of future 5G (and beyond) systems the radio channel will become more and more dynamic: Line-of-Sight (LoS) to Non-Line-of-Sight (NLoS) transitions will become more abrupt due to the lower diffraction contributions and Doppler shifts will increase proportionally to the carrier frequency.

Due to the large variety of possible environment and system configurations, accurate deterministic propagation models are essential for the design and simulation of vehicular communication systems. Moreover, since accurate Channel State Information (CSI) estimation is almost impossible in highly-dynamic scenarios, especially when beamforming is used, deterministic propagation models might be called to provide real-time estimates of the channel's characteristics or to help CSI estimation in future vehicular and/or mm-wave applications [1][8][10].

In the present work we present a "Dynamic Ray Tracing" (DRT) algorithm that can perform a deterministic ray-based prediction, including the computation of time delays and Doppler's shifts for each ray, with a single run using a proper representation of a dynamic environment where not only radio terminals, but also some of the environment's finite objects can move. The "dynamic environment database" contains the geometric description at a given snapshot time t_0 of a moving environment where vehicles, aircrafts etc., are described as polyhedrons moving in space with roto-translation vectors. With this approach, a single RT run can yield a multidimensional channel prediction starting from t_0 over the entire channel's multipath "coherence time" T_C, intended here as the lifetime of the overall multipath structure, i.e. of its major multipath components [11]. This means that, if the speed of each moving object doesn't change significantly over T_C, we can derive each path's Doppler shift and time-delay evolution with simple analytical formulas over T_C on the base of one single RT computation. A similar concept was presented in [8] and [9], where ray-based propagation models where applied to vehicular propagation with moving terminals and scatterers. In such investigations however the fact that reflection and diffraction points can actually slide over the obstacles' surfaces in a moving scene is disregarded. This is especially important in short-range applications with large obstacles such as buses, or when specular reflection from smooth walls (e.g. glass noise barriers) on the street side is considered.

In the present paper we present the DRT concept and show how the channel's multi-dimensional parameters – including Doppler's shifts – and their evolution over T_C can be derived with a single DRT run in a simple street-canyon environment.

The first results reported here show that realistic Power-Doppler-Profiles can be derived in a few reference configurations.

Further work will have to deal with the application of the approach to more complex scenarios and with its validation vs. measurements.

All the authors are with Department of Electrical, Electronic and Information Engineering, "G. Marconi" (DEI), University of Bologna, IT-40136 Bologna, Italy (e-mail: {denis.bilibashi2, enricomaria.vitucci, v.degliesposti}@unibo.it)

II. Algorithm description

The proposed DRT algorithm is based on a classical 3D image-based Ray Tracing approach, as described in [2]. The rays are traced according Geometrical Optics and the Uniform Theory of Diffraction, whereas diffuse scattering can be taken into account through the Effective Roughness model but is not considered here. An input database provides the description of the environment for a given instant in time t_0 where objects (buildings, vehicles etc.) are described as polyhedrons with flat surfaces and right edges. In addition to the geometric information of walls and objects with their electromagnetic material parameters, the instant velocity of each single moving object is also provided in the input database as a set of three elements: i) a translation vector, ii) a rotation center point, iii) a rotation vector. Moreover the speed vectors of transmitter (v_T) and receiver (v_R) are also specified.

This approach has two main advantages:

- Firstly, the Doppler information are computed online in the algorithm with the aid of simple formulas, as shown below. In such a way, there is no need to consider successive "snapshots" of the environment with slightly different displacements of the objects, and then to calculate the Doppler shifts with a "finite difference" computation method.

- Secondly, if we define T_C as the "coherence time" of the channel, i.e. the time during which the velocities are constant and the multipath structure remains unchanged, DRT prediction for time t_0 is still valid for an infinite number of snapshots in the interval $[t_0, t_0+T_C]$. This involves not only the Doppler information, but also the information in the angle and time-domain (e.g. Power-Delay Profiles).

•

When Tx and Rx are both moving, the resulting frequency including the Doppler shift is computed for the LoS ray using the following equation:

$$f' = f_0 \left(\frac{c - \vec{v}_R \cdot \hat{k}}{c - \vec{v}_T \cdot \hat{k}} \right) \quad (1)$$

where f_0 is the carrier frequency of the transmitted signal, $\hat{k}$ is a unit vector along the direction of the ray departing from the Tx towards the Rx, and v_T, v_R are the velocities of transmitter and receiver, respectively.

This formula can be extended in a straightforward way to rays with multiple bounces, where we have n scattering (bouncing) points, each one moving with a different speed (see Fig. 1):

$$f' = f_0 \cdot \prod_{i=1}^{n+1} \left(\frac{c - \vec{v}_i \cdot \hat{k}_i}{c - \vec{v}_{i-1} \cdot \hat{k}_i} \right) \quad (2)$$

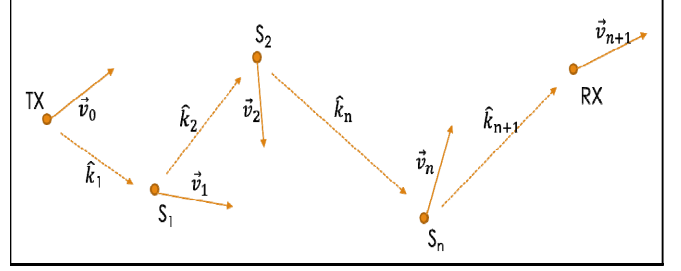A similar formulation was derived in [9] in iterative form.

Figure 1 – Representation of the multiple-scatterers Doppler model

Equation (2) assumes that the velocities of the interaction points on the objects are known. In the simplified case of small scattering objects that can be approximated as "point-scatterers" (e.g. drones or aircrafts far in the sky) no further processing is needed, and we can directly apply eq. (2).

Instead, in the case of large objects we need to compute the velocity of the reflection/diffraction points on the object surface.

Let's consider the typical vehicular case of a transmitter and a receiver both moving along a street canyon, whose side walls are modelled as flat reflecting surfaces. For example, in the case shown in Figure 2 (top view), we have Tx and Rx mounted on 2 vehicles moving along different street lanes in opposite directions, with speeds v_T and v_R, not necessarily parallel to each other, respectively.

Let's assume that the Tx and Rx positions at the instant t_0 are P_T and P_R (Fig. 2). After a time interval Δt, Tx and the corresponding image-Tx (i.e. the "virtual" transmitter, tagged as VP_T) will move from the initial positions to P_T' and VP_T', respectively, while the receiver will move to P_R'.

Assuming that Tx and Rx are at the same height above ground, this is a simple two-dimensional problem, and the instantaneous speed of the reflection point (v_Q) can be derived with simple geometric rules (see Fig. 2). In particular, v_Q can be computed through a finite differences method with the following equation:

$$\vec{v}_Q = \frac{dQ_R}{dt} = \lim_{\Delta t \to 0} \frac{Q_R' - Q_R}{\Delta t} \quad \text{where}: \begin{cases} Q_R = r \cap \pi \\ Q_R' = r' \cap \pi \end{cases} \quad (3)$$

where Q_R and Q_R' are the positions of the reflection point at the time instants t_0 and t_0+dt, respectively. These 2 points are computed by intersecting the reflecting wall plane π with r, and r', i.e the half lines connecting the Virtual Tx positions (VP_T ad VP_T') and the Rx positions (P_R, P_R'). The straight lines r and r' can be expressed through the following parametric equations:

$$r : VP_T + s \cdot \hat{u}$$

$$r' : VP_T' + s \cdot \hat{u}'$$

where s is a real positive parameter, and $\hat{u}$, $\hat{u}'$, are unit vectors pointing from the Virtual Tx towards the Rx position at the two time instants t_0 and t_0+dt:

$$s \in [0,+\infty] \quad \text{and} \quad \begin{cases} \hat{u} = \dfrac{P_R - VP_T}{\left|P_R - VP_T\right|} \\[2mm] \hat{u}' = \dfrac{P_R' - VP_T'}{\left|P_R' - VP_T'\right|} = \dfrac{(P_R + \vec{v}_R \Delta t) - (VP_T + \vec{v}_T \Delta t)}{\left|(P_R + \vec{v}_R \Delta t) - (VP_T + \vec{v}_T \Delta t)\right|} \end{cases}$$
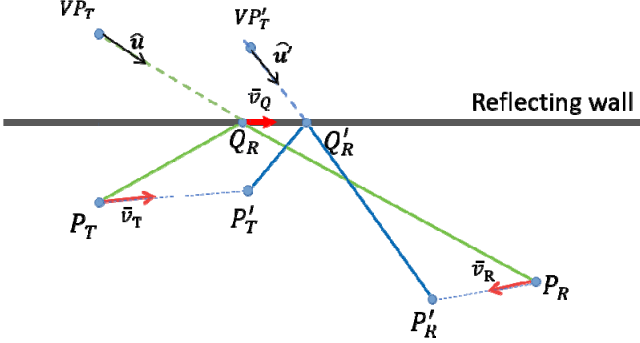

Figure 2 – Motion of the reflection point Q_R, when Tx and Rx are at the same height and moving with velocities $\mathbf{v}_T$, $\mathbf{v}_R$ arbitrarily oriented with respect to the reflecting surface (assumed static).

In the case depicted in Fig. 2, the reflection point will simply slide along the reflecting wall, since this wall is static.

To further extend the previous formulation, we now consider the reflection on a surface of a moving object (for example another vehicle driving on a different lane): in general, this object can have a roto-translational motion, described by the following equation:

$$\vec{v}_{obj} = \vec{v}_{trasl} + \vec{\omega}_{obj} \times \overrightarrow{OP} \tag{4}$$

where $\mathbf{v}_{trasl}$ is the translation speed of the object, O is the rotation center, $\vec{\omega}_{obj}$ is the angular speed, and P is the considered point of the object, assumed as a rigid body.

In order to take into account the object velocity, we can adopt a reference system integral with the moving object (e.g. with the origin located in the rotation center), and then compute the *relative* velocities of Tx and Rx.

By doing so, the relative velocities are computed through a velocity-addition formula [12] (i.e. adding vectors $\vec{v}_T$ and $\vec{v}_R$ to $\vec{v}_{obj}$) while the reflecting wall becomes static with respect to the new reference system, and Eq.(3) can be applied similarly to the static case, but using these relative velocities.

This formulation can be also applied to diffraction, with reference to the case shown in Fig.'s 2: for example, in the case of diffraction from the upper horizontal edge of the canyon sidewalls, the diffraction point will shift along the edge similarly to the reflection point. The case of diffraction on a vertical edge is even simpler: the diffraction point remains unchanged in the case of diffraction on a static object, while it moves in accordance with eq. (4) in the case of diffraction on a moving object.

Moreover by applying image theory, the considered formulation can be generalized in a straightforward way to a multiple-bounce case Some examples including multiple bounces and objects with roto-translational motion will be shown in the next Section. In the more general case of Tx / Rx with different heights, a 3D matrix formulation is needed to calculate the motion of the reflection point. This extension is not presented here for the sake of brevity, and will be described in future works.

Another important aspect is that, based on the same principle used to compute the instantaneous speed of the interaction points at a certain time, it is also possible to predict the behaviour of the channel in a subsequent instant without need to perform a new simulation, provided that the structure of the multipath is preserved, i.e. the major rays are the same, albeit moving in time. This "extrapolation" method is valid throughout the coherence time Tc, which is inversely proportional to the degree of mobility of the terminals and objects. The extrapolation method can be explained looking at Figure 2: if we know the position Q_R of the reflection point at t_0, and assuming that the Tx and Rx velocities have not changed, we can use the instantaneous velocity of the reflection point ($\mathbf{v}_Q$) already computed through eq. (2), and estimate the new location of the reflection point at $t_0+\Delta t$ as:

$$Q_R' = Q_R + \vec{v}_Q \Delta t \tag{5}$$

Then, we can instantaneously re-compute the ray trajectories (i.e. blue segments P_T'-Q_R'-P_R' in Fig. 2) without need of a new Ray Tracing run.

III. RESULT EXAMPLES

In this section we show some results obtained with the DRT approach in a simple vehicular environment composed of a street-canyon, a moving parallelepiped made of metal representing a bus, and two moving radio terminals (V2V environment).

The scene consists of an ideal street canyon which is 1 km long and has building walls on both sides, and two building walls closing its end sections, that can produce reflections with maximum Doppler shifts. Besides, the two vehicles carrying the Tx and Rx terminals drive on opposite lanes, while the bus is moving on a side lane, and therefore can generate a reflection from its side surface (Figure 3).
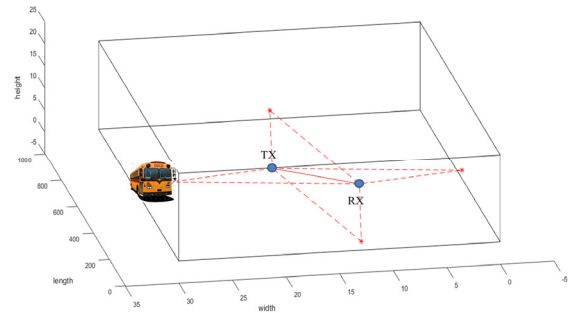

Figure 3 – Representation of the V2V Scenario, with LoS ray and single-bounce rays on the bus and canyon walls.

We considered an animation of the scene for a total time period T_P=11 seconds. Since T_P is greater than the coherence time in the considered scenario, we performed few DRT runs (one snapshot every 2 seconds), and for each of them we could

derive the Power Doppler-frequency Profile (PDfP) [13] in one single shot by applying equations (2), (3) and (4).

A further case with a bus rotation of π/6 [rad/s] is also considered, as if the bus were skidding toward the center lane.

A. Bus moving straight on a side lane: reflection from side

We first consider the Tx moving toward the end of the street canyon at 50 km/h while the bus and the Rx are moving in the opposite direction at 30 km/h and 36 km/h, respectively. Top views of the scenario for the first, the middle and the last snapshots of the scene are shown in Figures 4.a, 4.b, 4.c, respectively. The bus is on a side lane and therefore generates a single-bounce reflection for a small fraction of the time period T_P. The 3D histogram in Figure 5 shows the evolution of the PDfP over T_P and discretized with a Doppler frequency step of 14.35 Hz. DRT simulations are performed with a maximum of 2 bounces.

The main contributions to the PDfP (LoS, single and double reflections) are also tagged in the plot. The most evident contributions are the direct ray, with a positive Doppler shift in the first part of the scene that becomes negative in the last part, after the Rx passes by the Tx (Fig. 4b) and the reflections from the sides of the street canyon, which generate Doppler shifts with the same trend as the direct ray but with lower values and a less abrupt transition. Contributions of reflections from the walls at the beginning and at the end of the street canyon are also evident.
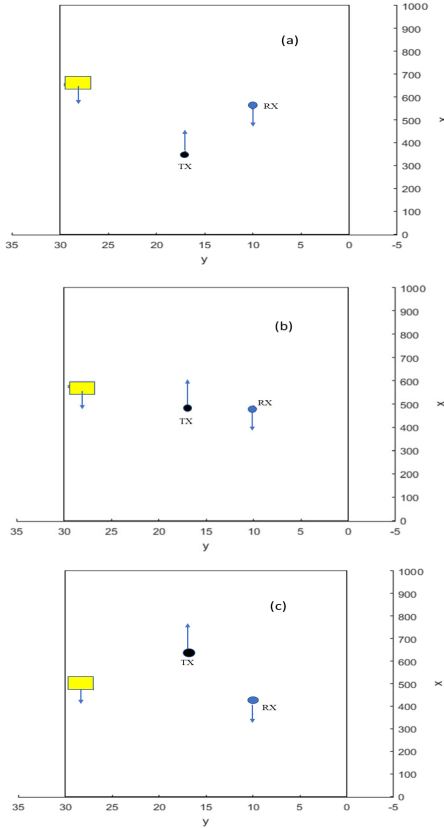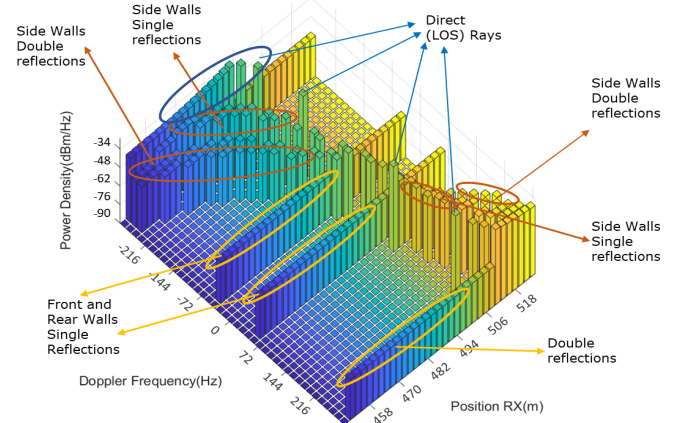

Figure 5 – PDfP evolution in a V2V scenario with a simulation time of 11 seconds (simulation with a maximum 2 bounces). Bus moving straight without rotation here.
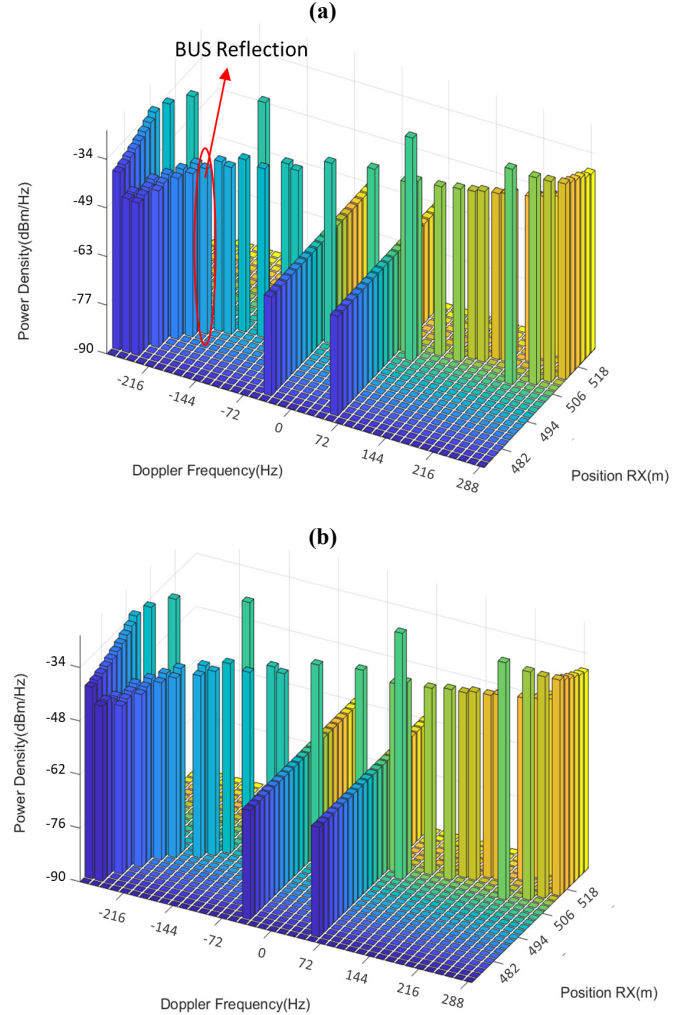

Figure 6 – PDfP evolution in a V2V scenario with a simulation time of 6 seconds. Bus moving straight without rotation here. (a) PDfP achieved performing multiple DRT runs (bus reflection is present). (b) PDfP achieved through extrapolation (bus reflection is missing here). Only single bounces are considered here.

Figure 4 – Start (a), mid (b) and end (c) scene snapshots for the V2V scenario

In Figure 6 we show the comparison between a PDfP obtained through multiple runs (Fig. 6a), and the same PDfP obtained through extrapolation of the ray paths according to eq. (5) (Fig. 6b). Only single bounces are considered here, for legibility reasons. In this case T_P is limited to 6 seconds: since this value is close to the coherence time limit, the two plots look almost identical, except for a contribution due to a single reflection on the bus sidewall. The extrapolation method is not able to catch the bus reflection, as this path was not present in the initial configuration, and therefore this contribution is missing in Fig. 6b.

B. *Bus moving straight on a side lane and then rotating*

We consider now the case of Tx and Rx moving in the same direction at 28 km/h and 30 km/h, respectively, while the bus is moving in the opposite direction at 30 km/h. A detail of the PDfP when bus reflection is present is shown in Figure 7 for the case of the bus driving straight (blue lines) and of the bus skidding toward the center lane (red lines), respectively. In the latter case the Doppler's shift of bus reflection becomes positive (37 Hz) due to the reflection point's movement toward the center lane.

This behavior is important from the applications point of view: when the Doppler frequency of a major multipath component abruptly changes, this could indicate a potentially dangerous situation, e.g. a vehicle swerving from its lane.
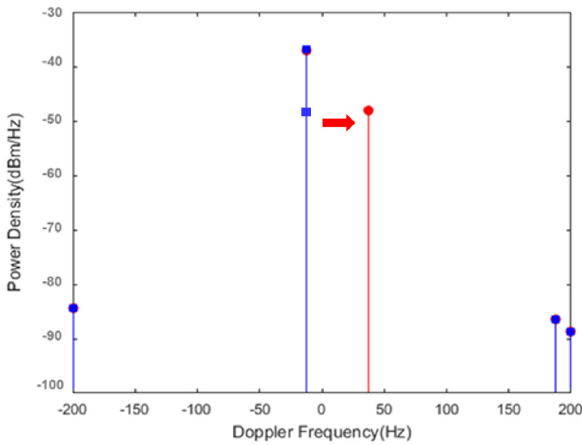

Figure 7 – PDfP for a snapshot of the V2V scenario with reflection from bus side. Here Tx and Rx are moving in the same direction at 28 km/ and 30 km/h, respectively, while bus is moving at 30 km/h in the opposite direction. Bus moving straight without (blue) and with (red) rotation.

IV. CONCLUSIONS

A "dynamic ray tracing" algorithm that can perform a deterministic ray-based prediction, including the computation of Doppler's shifts for each ray with a single run using a proper representation of a dynamic environment, is presented. The "dynamic environment database" contains the geometric description at a given snapshot time t_0 of a moving environment where vehicles are described as polyhedrons moving in space using roto-translation vectors.

In the present paper we describe the dynamic ray tracing concept and its formulation for a simple street-canyon environment with moving radio terminals and a large moving vehicle representing a bus or a truck. Results show that realistic power-Doppler profiles can be derived for different reference cases and with a very limited number of ray tracing runs, thanks to the possibility of extrapolating the path geometries within the coherence time.

Further work will have to deal with validation of the model vs. measurements and with its application to more complex scenarios and to specific link-level or systems level simulations.

REFERENCES

[1] Z. Yun and M. F. Iskander, "Ray Tracing for Radio Propagation Modeling: Principles and Applications," in IEEE Access, vol. 3, pp. 1089-1100, 2015.

[2] F. Fuschini, E. M. Vitucci, M. Barbiroli, G. Falciasecca and V. Degli-Esposti, "Ray tracing propagation modeling for future small-cell and indoor applications: A review of current techniques," in Radio Science, vol. 50, no. 6, pp. 469-485, June 2015.

[3] S. Chen et al., "Vehicle-to-Everything (V2X) Services Supported by LTE-Based Systems and 5G," in IEEE Communications Standards Magazine, vol. 1, no. 2, pp. 70-76, 2017.

[4] H. Wymeersch, G. Seco-Granados, G. Destino, D. Dardari and F. Tufvesson, "5G mmWave Positioning for Vehicular Networks," in IEEE Wireless Communications, vol. 24, no. 6, pp. 80-86, Dec. 2017.

[5] R. S. Thomae et al., "Cooperative Passive Coherent Location: A Promising 5G Service to Support Road Safety," in IEEE Communications Magazine, vol. 57, no. 9, pp. 86-92, September 2019.

[6] A. Molisch, F. Tufvesson, J. Karedal, and C. Mecklenbräuker, "A survey on vehicle-to-vehicle propagation channels," IEEE Wireless Commun., vol. 16, no. 6, pp. 12–22, 2009.

[7] W. Viriyasitavat, M. Boban, H. Tsai and A. Vasilakos, "Vehicular Communications: Survey and Challenges of Channel and Propagation Models," in IEEE Vehicular Technology Magazine, vol. 10, no. 2, pp. 55-66, June 2015.

[8] L. Azpilicueta, C. Vargas-Rosales and F. Falcone, "Intelligent Vehicle Communication: Deterministic Propagation Prediction in Transportation Systems," in IEEE Vehicular Technology Magazine, vol. 11, no. 3, pp. 29-37, Sept. 2016.

[9] F. Wiffen, L. Sayer, M. Z. Bocus, A. Doufexi and A. Nix, "Comparison of OTFS and OFDM in Ray Launched sub-6 GHz and mmWave Line-of-Sight Mobility Channels," 2018 IEEE 29th Annual International Symposium on Personal, Indoor and Mobile Radio Communications (PIMRC), Bologna, 2018, pp. 73-79

[10] F. Fuschini, M. Zoli, E.M. Vitucci, M. Barbiroli and V. Degli-Esposti, "A Study on Mm-wave Multi-User Directional Beamforming Based on Measurements and Ray Tracing Simulations," IEEE Transactions on Antennas and Propagation, Vol 67, No. 4, pp 2633-2644, April 2019.

[11] H. M. El-Sallabi, H. L. Bertoni and P. Vainikainen, "Experimental evaluation of RAKE finger life distance for CDMA systems," in IEEE Antennas and Wireless Propagation Letters, vol. 1, pp. 50-52, 2002.

[12] H. Goldstein, *Classical Mechanics*, Pearson Education, 2014.

[13] J. D. Parsons, *The Mobile Radio Propagation Channel*, Wiley, Chichester, U. K., 2000.